# Two- and three-photon absorption cross-section characterization for high-brightness, cell-specific multiphoton fluorescence brain imaging

Aleksandr A. Lanin[1,3] | Artem S. Chebotarev[1] | Matvei S. Pochechuev[1,4] | Ilya V. Kelmanson[5,6] | Daria A. Kotova[5] | Dmitry S. Bilan[5,6] | Yulia G. Ermakova[5,7] | Andrei B. Fedotov[1,3] | Anatoly A. Ivanov[1,8] | Vsevolod V. Belousov[5,6] | Aleksei M. Zheltikov[*,1,2,3,4]

1 Physics Department, International Laser Center, M.V. Lomonosov Moscow State University, Moscow 119992, Russia

2 Department of Physics and Astronomy, Texas A&M University, College Station TX 77843, USA

3 Russian Quantum Center, ul. Novaya 100, Skolkovo, Moscow Region, 143025 Russia

4 Kurchatov Institute National Research Center, Moscow 123182, Russia

5 M.M. Shemyakin and Yu.A. Ovchinnikov Institute of Bioorganic Chemistry, Russian Academy of Sciences, Moscow 117997, Russia

6 Pirogov Russian National Research Medical University, Moscow 117997, Russia

7 European Molecular Biology Laboratory, Heidelberg 69117, Germany

8 Center of Photochemistry, Crystallography and Photonics Federal Research Center, Russian Academy of Sciences, ul. Novatorov 7a, Moscow 119421, Russia

*** Correspondence**

Aleksei M. Zheltikov, Physics Department, International Laser Center, M.V. Lomonosov Moscow State University, Moscow 119992, Russia

Email: zheltikov@physics.msu.ru

We demonstrate an accurate quantitative characterization of absolute two- and three-photon absorption (2PA and 3PA) action cross sections of a genetically encodable fluorescent marker Sypher3s. Both 2PA and 3PA action cross sections of this marker are found to be remarkably high, enabling high-brightness, cell-specific two- and three-photon fluorescence brain imaging. Brain imaging experiments on sliced samples of rat's cortical areas are presented to demonstrate these imaging modalities. The 2PA action cross section of Sypher3s is shown to be highly sensitive to the level of pH, enabling pH measurements via a ratiometric readout of the two-photon fluorescence with two laser excitation wavelengths, thus paving the way toward fast optical pH sensing in deep-tissue experiments.

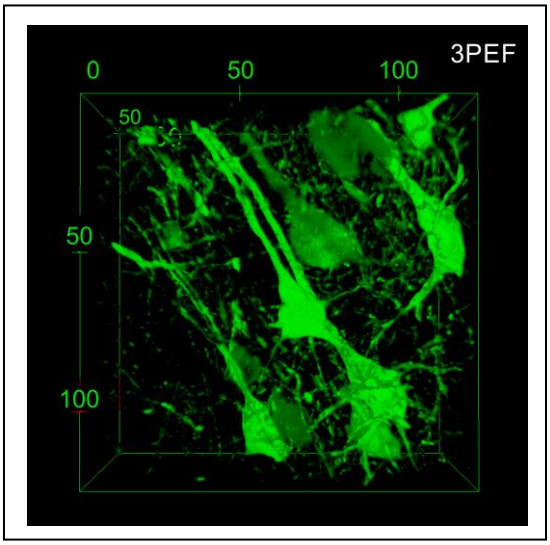


**KEYWORDS**
two-photon microscopy, three-photon microscopy, fluorescent biosensors, brain imaging

## 1 | INTRODUCTION

As one of its fundamental results, perturbative nonlinear optics relates the cross section of $n$-photon absorption $\sigma_n$ to the imaginary part of the pertinent nonlinear susceptibility $\chi^{(n+1)}$ [1]. In a lossless nonlinear medium, effects related to $(n + 1)$-photon absorption are therefore bound to be much weaker than effects caused by $n$-photon absorption. The strong-scattering regime is, however, a very different matter. Surprising as it may seem from the standpoint of the fundamentals of nonlinear optics, fluorescence excited via three-photon absorption (3PA) deep inside a strongly scattering biological object [2] is often more intense than two-photon-excited fluorescence (2PEF). In their seminal work, Horton et al. (Ref. [3]) have shown that microscopy based on three-photon-excited fluorescence (3PEF) enables a noninvasive, high-resolution *in vivo* imaging of subcortical structures within an intact mouse brain. Significant recent milestones in the development of 3PEF imaging technology include demonstration of optical imaging of neuronal activity deep in intact mouse brain [4], wide-field three-photon optogenetic stimulation [5], brain structure and function detection through an intact skull [6], and 3PEF light-sheet microscopy [7].

The key to understand this counterintuitive relation between the 2PEF and 3PEF intensities in multiphoton bioimaging is the wavelength-dependent loss of biological systems, which can be, in its turn, traced back to the wavelength-dependent scattering and absorption of the main constituents of biological tissues – water, blood, melanin, and fat. The laser wavelength $\lambda_0$ required for an efficient fluorescence excitation through a suitable electronic transition of a fluorophore is, roughly, 3/2 time longer than $\lambda_0$ required for two-photon fluorescence excitation via the same transition. For typical dipole-allowed electron transitions of many

This article has been accepted for publication and undergone full peer review but has not been through the copyediting, typesetting, pagination and proofreading process which may lead to differences between this version and the Version of Record. Please cite this article as doi:10.1002/jbio.201900243

widespread fluorophores, three-photon excitation can be achieved with $\lambda_0 > 1.2 - 1.3$ μm [2]. Within this range of wavelengths, laser radiation is much less prone to attenuation due to the joint effect of absorption and scattering in a biological tissue than at around 800 nm – the range of wavelengths at which the short-pulse output of a standard Ti: sapphire laser source hits a two-photon resonance with an electronic transition of a fluorophore.

Since all the remarkable bioimaging capabilities of 3PEF are achieved at the cost of a higher order of optical nonlinearity, a compromise between the 3PEF intensity and the multiphoton ionization rate is often reached at the level of laser intensities that often raises concerns [8–11] regarding an increased risk of unwanted photoinduced changes in functions of a biological system. Central to the question as to whether such unwanted photobiological effects can be avoided without sacrificing too much of the 3PEF signal is the 3PA action cross section $\varphi\sigma_3$, with $\varphi$ being the fluorescence yield. An accurate quantitative characterization of this parameter needs to be performed in a well-controlled experiment in a solution without any unnecessary loss or scattering [2, 12, 13]. In this regime, the 3PEF intensity is many orders of magnitude lower than the 2PEF intensity, making an accurate quantitative measurement of the action cross section $\varphi\sigma_3$ as a function of the wavelength extremely difficult. As a significant milestone on the way toward establishing the methodology of such measurements, Rebane and Mihaylov (Ref. [14]) have recently reported carefully measured $\sigma_3$ spectra for a variety of widespread dyes, Rhodamine 6G among them, thus providing a much-needed reference for a quantitative $\varphi\sigma_3$ characterization of candidate chromophores potentially promising for 3PEF imaging. Here, we use these earlier results by Rebane and Mihaylov as a reference for a quantitative characterization of two- and three-photon absorption action cross sections of a genetically encodable fluorescent marker Sypher3s. Both 2PA and 3PA action cross sections of this marker are found to be remarkably high, enabling high-brightness, cell-specific two- and three-photon fluorescence brain imaging. Brain imaging experiments on sliced samples of rat's cortical areas are presented to demonstrate these imaging modalities.

## 2 | EXPERIMENTAL

Both multiphoton-absorption characterization and brain imaging experiments were performed on a versatile laser platform integrating Ti: sapphire and Cr: forsterite and short-pulse laser sources (Fig. 1). The Ti: sapphire laser used in our studies delivers ≈80-fs pulses with a central wavelength $\lambda_0$ tunable from ≈ 700 to 980 nm and an energy up to 30 nJ at a pulse repetition rate of 76 MHz. These pulses drive an optical parametric oscillator (OPO), based on a periodically poled potassium titanyl phosphate (PPKTP) crystal, whose chirped-pulse output is tunable within the range of wavelengths $\lambda_0$ from ≈ 980 to 1500 nm, with the output pulse width varying within this tunability range from ≈ 350 to 500 fs. The OPO output is used for two-photon absorption characterization, as well as for the optical excitation of 2PEF in brain imaging. An in-house-built extended-cavity, ytterbium-fiber-laser-pumped Cr: forsterite laser [15] is set to generate ≈60-fs laser pulses at a central wavelength $\lambda_0 \approx 1.25$ μm with an energy up to 25 nJ and a pulse repetition rate of about 30 MHz, providing a short-pulse near-infrared pump for three-photon absorption characterization, as well as a short-pulse source for 3PEF brain imaging.

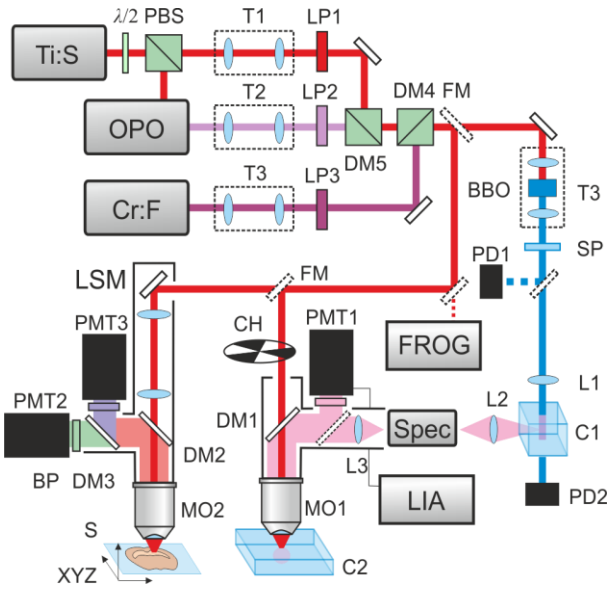


**FIGURE 1** Experimental setup for multiphoton absorption cross section measurements: Ti: S, Ti: Sapphire laser; Cr: F, Cr: Forsterite laser; OPO, optical parametric oscillator; LSM, laser scanning microscope; Spec, spectrometer; FROG, frequency-resolved optical gating apparatus; LIA, lock-in amplifier; PMT1 – PMT3, photomultipliers; T1 – T4, telescopes; CH, optical chopper; LP1 – LP3, longpass filters; SP, shortpass filter, BP, bandpass filter; DM1 – DM5, dichroic mirrors; FM, flip mirror; PD1, PD2, photodiodes; MO1, MO2, microscope objectives; L1 – L3, lenses; BBO, Beta barium borate nonlinear crystal; XYZ, three-dimensional stage; C1, C2, cells with a fluorophore sample; S, brain slice.

The spectrum of one-photon-excited fluorescence (1PEF) is recorded in our experimental arrangement from the first cell with a sample solution, which is irradiated by the ≈432-nm second-harmonic output of the BBO crystal. These measurements are used for an accurate calibration of fluorophore concentration in a sample. The 2PEF and 3PEF signals, driven by near-IR Ti: sapphire and Cr: forsterite laser beams, focused with an infrared-grade, long-working-range 50x/0.65 microscope objective, are generated in the second sample cell. Both signals are then bandpass-filtered in their respective channels for a higher detection contrast to be spectrally analyzed with a spectrometer. As an additional resource in the characterization of weak 3PEF signals from diluted fluorescent marker samples, the fluorescence signal bandpass-filtered within a 40-nm band centered at ≈520 nm is detected with a photomultiplier, followed by a lock-in amplification. Combined with an optical chopper, modulating the laser pump at ≈860 Hz, and a lock-in amplification of the signal from the photomultiplier, this approach enables noise suppression below 200 nV even for the maximum current gain of the photomultiplier.

The fluorescent system chosen for our study, Sypher3s, has been originally designed as a genetically encodable, enhanced-brightness fluorescent pH sensor, [16] providing a nearly order-of-magnitude enhancement in fluorescence brightness relative to the original forms of Sypher [17]. The excitation spectrum of Sypher3s features two peaks [16], centered at ≈ 410 and 495 nm, corresponding to protonated and nonprotonated forms of the chromophore, enabling the detection of fast intracellular pH dynamics in a vast class of biological systems, ranging from cellular subcompartments to regenerating animal tissues [16]. As recent experiments have shown [18], Sypher3s can serve as a high-brightness fluorescent marker for cell-specific, subcellular resolution multiphoton brain imaging. When used as a part of a suitable gene-delivery virus construct under a control of appropriate promoter, to target the chosen type of cells, Sypher3s provides a highly efficient, highly specific targeting to the chosen type of cells [19, 20].

## 3 | RESULTS AND DISCUSSION

In Fig. 2a, we present 1PEF, 2PEF, and 3PEF spectra of Sypher3s in a phosphate-buffered saline (PBS) solution with a concentration of Sypher3s $C_s \approx 9.4\ 10^{-6}$ M and pH ≈ 7.4. One-, two-, and three-photon excitation in this experiment is provided by, respectively, the 432-nm second harmonic of Ti: sapphire laser radiation, the 865-nm fundamental-wavelength output of the Ti: sapphire laser, and the 1250-nm pulses delivered by the Cr: forsterite laser. We emphasize that Fig. 2a shows fluorescence, not excitation spectra, with the detection rather than excitation wavelength along the abscissa axis. All three spectra are almost indistinguishable from each other, featuring a well pronounced peak centered at $\lambda_f \approx 515$ nm. While the 1PEF signal grows linearly with the laser power $p$, the 2PEF and 3PEF intensities are nonlinear functions of the laser power, closely following the $p^2$ and $p^3$ scaling (Fig. 2b), indicating that, when driven by the 865-nm output of the Ti: sapphire laser and the 1250-nm output of the Cr: forsterite laser, fluorescence excitation occurs exclusively via 2PA and 3PA pathways, respectively.

Central to absolute multiphoton absorption action cross section measurements is an accurate calibration of the $n$-photon fluorescence spectra, such as those shown in Fig. 2a, against the spectral dependences of $\varphi\sigma_n$ for a reference fluorescent system. While for two-photon absorption (2PA), such reference data have been available for more than a decade [2, 21], the reference standards for 3PA cross sections have been established only recently [14]. Here, we use these earlier measurements for $\sigma_2$ and $\sigma_3$ of Rhodamine 6G [14, 21] as a reference to define the 2PA and 3PA action cross sections for Sypher3s and follow the referencing procedure as described by Makarov et al. (Ref. [21]).

Fluorescent samples for reference measurements were prepared by dissolving Rhodamine 6G crystals in ethanol to a Rhodamine 6G concentration $C_r \approx 5.8\ 10^{-5}$ M. The 1PEF, 2PEF, and 3PEF spectra of this reference sample are presented in Fig. 2a. With the power of 865-nm laser

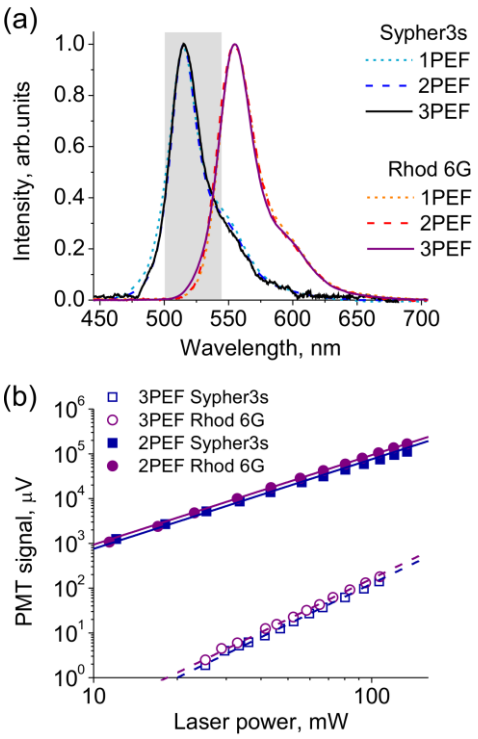


**FIGURE 2** (a) 1PEF (dotted lines), 2PEF (dashed lines), and 3PEF (solid lines) spectra of Sypher3s (blue, navy, and black lines) and Rhodamine 6G (orange, red, and purple lines). Gray shading shows the spectral range (≈ 500 to 540 nm) within which the fluorescence signal is bandpass-filtered in 2PEF and 3PEF measurements. The 432-nm second-harmonic output of the Ti: sapphire laser, 865-nm fundamental-wavelength output of the Ti: sapphire laser, and the 1250-nm output of the Cr: forsterite laser are used for one-, two-, and three-photon excitation, respectively. (b) The 2PEF (filled circles and boxes) and 3PEF (open circles and boxes) readout from Sypher3s (boxes) and Rhodamine 6G (circles) as a function of the laser power $p$. The 865-nm output of the Ti: sapphire laser and the 1250-nm output of the Cr: forsterite laser are used for two- and three-photon excitation, respectively. Also shown are the best $p^2$ (solid lines) and $p^3$ (dashed lines) fits.

excitation set at $p \approx 44$ mW, the lock-in amplifier output reading is 17.5 ± 0.1 mV for the Rhodamine 6G 2PEF signal and 15.7 ± 0.2 mV for the 2PEF from a PBS Sypher3s solution with $C_s \approx 9.4\ 10^{-6}$ M and pH ≈ 7.4 – a level of pH typical for biological tissues and blood plasmas. The dark-current noise of the detector in these measurements never exceeded 200 nV. With a 2PA action cross section of Rhodamine 6G estimated as $(\varphi\sigma_2)_r \approx 8.6$ GM [21], these measurements lead to $\varphi\sigma_2 \approx 8.2$ GM (1 GM = $10^{-50}$ cm$^4$s) for the 2PA action cross section of Sypher3s at $\lambda_e \approx 865$ nm. The 3PEF from the same Rhodamine 6G and Sypher3s samples irradiated by laser pulses with $\lambda_e \approx 1250$ nm and $p \approx 52$ mW yields a voltage of, respectively, 22.7 ± 0.4 μV and 18.2 ± 0.4 μV at the output of the lock-in amplifier. With a $(\varphi\sigma_3)_r \approx 2.85\ 10^{-81}$ cm$^6$ s$^2$ estimate for Rhodamine 6G [14], the 3PA action cross section of Sypher3s at this excitation wavelength is at $\varphi\sigma_3 \approx 2.3\ 10^{-81}$ cm$^6$ s$^2$.

In Fig. 3a, we present the 2PA action cross sections of Rhodamine 6G and Sypher3s measured as functions of the laser excitation wavelength. For Rhodamine 6G, the spectral

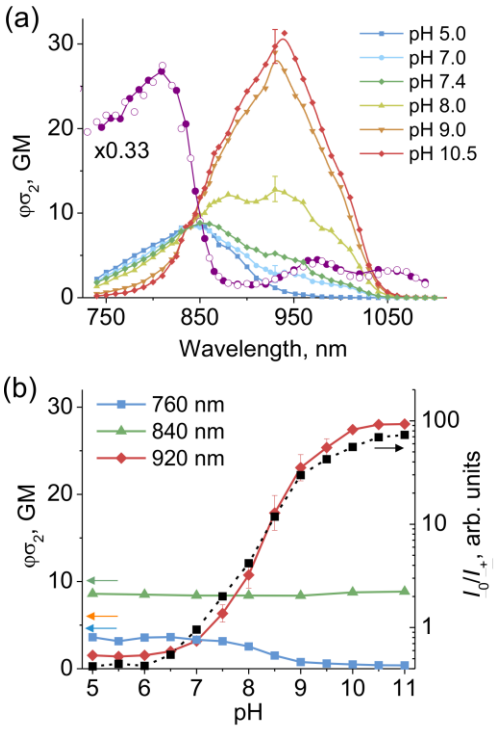


**FIGURE 3** (a) The 2PA action cross section of Sypher3s measured as a function of the laser excitation wavelength with pH varying from ≈ 5.0 to 10.5. Also shown is the 2PA action cross section of Rhodamine 6G as a function of the laser excitation wavelength as measured in our experiments (filled circles) and as provided in Ref. 21 (open circles). Note a 0.5 multiplier for the 2PA action cross sections of Rhodamine 6G. (b) The 2PA action cross section of Sypher3s measured as a function of the pH level in the PBS solution of Sypher3s for $\lambda_e \approx 760$ nm (blue boxes), 840 nm (green triangles), and 920 nm (red diamonds). Also shown (black boxes, right axis, log scale) is the pH dependence of the ratio $I_0/I_+$ of the intensity $I_0$ of 2PEF excited at $\lambda_e = 920$ nm to the intensity $I_+$ of 2PEF driven at $\lambda_e = 760$ nm.

dependence of the 2PA action cross section determined in our experiments is seen to closely follow the spectral dependence of $\varphi\sigma_2$ as defined in earlier studies [21], thus verifying our measurements. For pH ≈ 7.4, the level of pH typical for biological tissues and blood plasmas, maximum $\varphi\sigma_2$ values are achieved in the range of wavelengths from ≈ 830 to 870 nm, showing that Sypher3s is ideally suited for TPA-based bioimaging with a mode-locked Ti: sapphire laser as a short-pulse excitation source.

The behavior of the TPA action cross sections for laser excitation wavelengths $\lambda_e$ shorter than ≈ 840 nm drastically differs from the behavior of $\varphi\sigma_2$ for $\lambda_e > 840$ nm (Figs. 3a, 3b). This property of $\varphi\sigma_2$ correlates well with the behavior of one-photon-excited fluorescence of Sypher3s [16]. Similar to its one-photon counterpart, the spectral dependence of the 2PEF of Sypher3s suggests the existence of two peaks in its two-photon excitation spectrum. As the level of pH in the solution rises, the 2PEF driven by laser pulses with $\lambda_e < 840$ nm becomes weaker (Figs. 3a, 3b). The 2PEF excited by laser radiation with $\lambda_e > 840$ nm exhibits an opposite behavior, rapidly growing in its brightness with increasing pH. Remarkably, at pH ≈ 10.5, the 2PA action cross section of

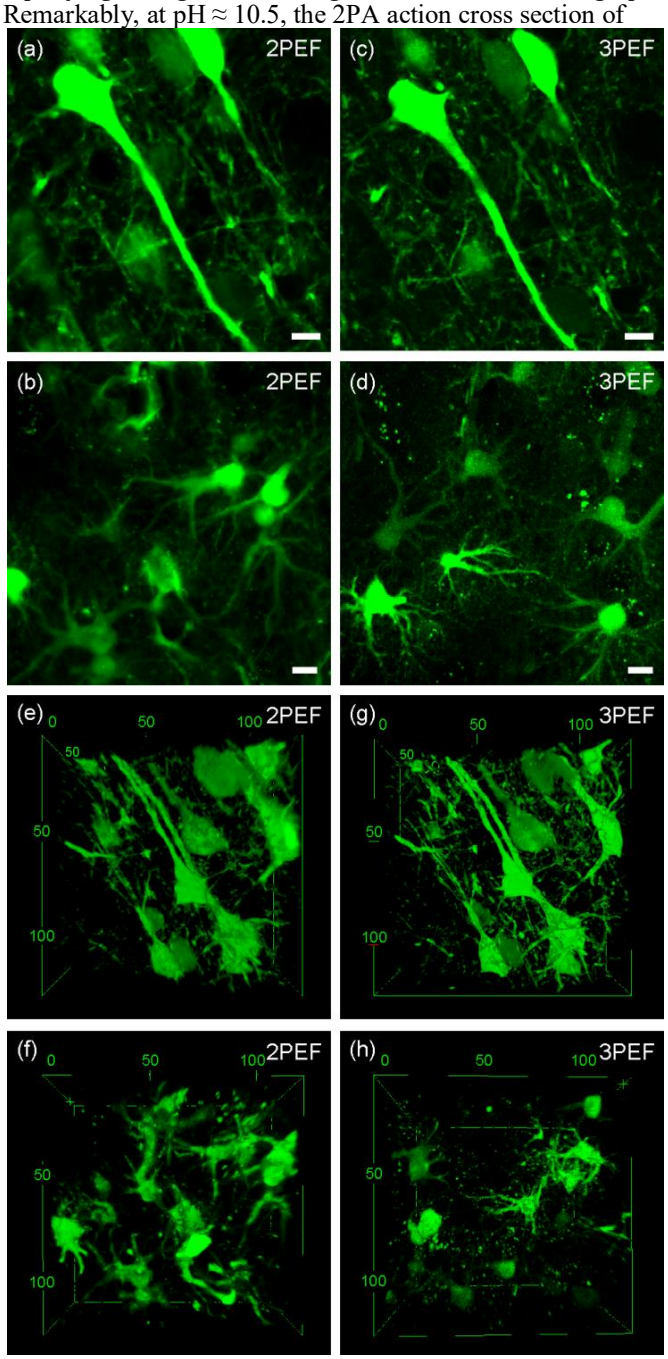


**FIGURE 4** (a – d) Typical 2PEF (a, b) and 3PEF (c, d) images taken inside rat's cortex with SypHer3s expressing in neurons (a, c) and astrocytes (b, d). 2PEF and 3PEF are driven by 870-nm and 1250-nm pulses, respectively. The scale bar is 10 μm. (e – h) Still views of 3D reconstruction (Multimedia view) of SypHer3s-expressing neurons (e, g) and astrocytes (f, h) from stacks of 2PEF (e, f) and 3PEF (g, h) images taken by scanning the focus of the laser beam with a 0.5-μm step along the z-axis inside rat's cortex. Full 3D reconstructions are presented as movies in supplemental files (Multimedia view).

Sypher3s excited at $\lambda_e \approx 940$ nm becomes as high as $\varphi\sigma_2 \approx 31$ GM (red diamonds in Fig. 3a). For comparison, the 2PA

action cross section of EGFP at the same excitation wavelength is $\varphi\sigma_2 \approx 30$ GM [13].

As lower pH values translate into higher chromophore protonation degrees, an increase in the brightness of 2PEF driven by laser pulses with $\lambda_e < 840$ nm provides a clear indication of the buildup of the protonated form of the chromophore. In the opposite limit of high pH, the spectral dependence of $\varphi\sigma_2$ of Sypher3s is seen to closely follow the spectral dependence of the 2PA action cross section for YFP. An isosbestic-point-like feature at $\lambda_e \approx 840$ nm (Figs. 3a, 3b) suggests that the overall 2PEF signal is a sum of two and only two components, identified as Sypher3s with protonated and nonprotonated forms of chromophore.

To provide a quantitative measure of pH in a medium, we introduce the ratio $I_0/I_+$ of the intensity $I_0$ of 2PEF excited at $\lambda_e = 920$ nm to the intensity $I_+$ of 2PEF driven at $\lambda_e = 760$ nm. As the level of pH increases from 5 to 11, the $I_0/I_+$ ratio increases by a factor of ≈ 180 (black boxes in Fig. 3b), enabling an accurate measurement of the pH level in the system. Our experiments thus demonstrate that the method of fast pH sensing based on a measurement of fluorescence intensity ratio for two laser excitation wavelengths [16] can be extended to two-photon-excited fluorescence, paving the way toward fast pH sensing in deep-tissue experiments.

Remarkably high 2PA and 3PA action cross sections of Sypher3s suggest that this fluorescent marker is ideally suited for high-brightness, cell-specific two- and three-photon deep-brain imaging. To demonstrate such imaging modalities, 2PEF and 3PEF experiments were performed on sliced samples of rat's cortical areas. Brain slice samples used in these studies were extracted from 10-week-old, male Wistar-line rats, purchased from the Pushchino Animal Breeding Center. For neuron or astrocyte staining, 1 μl of AAV9-hSyn1-Sypher3s or AAV9-GFAP-Sypher3s, encoding Sypher3s fluorescent reporter under the control of, respectively, a human synapsin 1 (hSyn1) or glial fibrillary acidic protein (GFAP) promoter was injected into rat's cortex (–1 mm dorsoventral from the brain surface) using a 5-μl Hamilton syringe with a 33-gauge needle. When combined with gene delivery via an appropriate adeno-associated virus (AAV) serotype, both promoters provide a highly efficient, highly specific targeting the chosen type of cells [19, 20]. Three weeks after the virus injection, the rats were euthanized, their brain was fixed for 24 hours in 4% paraformaldehyde solution in protein-free phosphate-buffered saline (PBS) and sliced into ≈2-mm-thick coronal sections.

For high-resolution imaging, the Cr: forsterite- and Ti: sapphire-laser beams are focused into a brain slice in an upright-microscopy scheme with a water-immersion 20x, NA = 1.00 near-IR objective. The fluorescence signal is bandpass-filtered within a wavelength range of 500 – 540 nm and detected by a photomultiplier. In Figs. 4a – 4d, we present 2PEF and 3PEF images taken at a depth of 370 μm inside rat's cortex with Sypher3s expressing in neurons. Due to its high 3PA action cross section, Sypher3s yields a 3PEF signal that is intense enough, as can be seen from Figs. 4c and 4d, to make Sypher3s-stained neurons readily visible in 3PEF images. As a general tendency, seen from the 2PEF and 3PEF images in 3a – 3d, 3PEF images are much sharper and show a much higher contrast compared to their 2PEF counterparts. This finding agrees well with the earlier three-photon imaging studies [3–7].

Figures 4e – 4h display still views of 3D reconstruction (Multimedia view) of Sypher3s-expressing neurons (Figs. 4e, 4g) and astrocytes (Figs. 4f, 4h) from stacks of 2PEF (e, f) and 3PEF (Figs. 4g, 4h) images taken by scanning the focus of the laser beam with a 0.5-μm step along the *z*-axis inside rat's cortex. Here, once again, a tighter confinement of the 3PEF signal translates into sharper cell images. Moreover, the improved optical sectioning capability provided by 3PEF microscopy helps detect and resolve, as comparison of 2PEF and 3PEF images in Fig. 4 shows, finer details in the structure and morphology of neurons and astrocytes. The ability of 3PEF to image subcellular structural features that cannot be detected by 2PEF microscopy can be further enhanced by exploiting the difference in selection rules inherent in 2PA and 3PA processes. Indeed, since 2PA and 3PA transitions couple the initial quantum state of a molecule to excited states with different symmetry properties, some of the excitation pathways prohibited in 2PA will be allowed in 3PA and can contribute to 3PEF. As a promising direction for future research, strategies of quantum control [22], used jointly with molecular design methods extended to genetically encodable fluorescent probes, can provide this currently missing pathway selectivity, further enhancing the contrast and spatial resolution of 3PEF microscopy.

## 4 | CONCLUSION

To summarize, we have demonstrated an accurate quantitative characterization of absolute two- and three-photon absorption action cross sections of a genetically encodable fluorescent marker Sypher3s. Both 2PA and 3PA action cross sections of this marker have been found to be high enough to enable high-brightness, cell-specific two- and three-photon fluorescence brain imaging. Brain imaging experiments on sliced samples of rat's cortical areas have been presented to demonstrate these imaging modalities. Moreover, the 2PA action cross section of Sypher3s has been shown to be highly sensitive to the level of pH in a medium, enabling pH measurements via a ratiometric readout of the two-photon fluorescence with two laser excitation wavelengths, thus paving the way toward fast optical pH sensing in deep-tissue experiments.


### ACKNOWLEDGEMENTS

This research was supported in part by the Russian Foundation for Basic Research (project nos. 17-00-00217, 18-29-20031, 18-52-00025) and Welch Foundation (Grant No. A-1801-20180324). Research by A.A.L. and A.S.C. into nonlinear microspectroscopy was supported by the Russian Science Foundation (project no. 18-72-10094). Research by A.M.Z., A.A.L., and M.S.P. into short-pulse sources for nonlinear imaging was supported by the Russian Science Foundation (project no. 17-12-01533).


### REFERENCES


[1] Y.R. Shen, *Principles of nonlinear optics*, Wiley-Interscience, New York, **1984**.

[2] C. Xu, W. Zipfel, J. B. Shear, R. M. Williams, W. W. Webb, *Proc. Natl. Acad. Sci.* **1996**, *93*, 10763.

[3] N. G. Horton, K. Wang, D. Kobat, C. G. Clark, F. W. Wise, C. B. Schaffer, C. Xu, *Nat. Photonics* **2013**, *7*, 205.

[4] D. G. Ouzounov, T. Wang, M. Wang, D. D. Feng, N. G. Horton, J. C. Cruz-Hernández, Y.-T. Cheng, J. Reimer, A. S. Tolias, N. Nishimura, *Nat. Methods* **2017**, *14*, 388.
[5] C. J. Rowlands, D. Park, O. T. Bruns, K. D. Piatkevich, D. Fukumura, R. K. Jain, M. G. Bawendi, E. S. Boyden, P. T. So, *Light Sci. Appl.* **2017**, *6*, e16255.
[6] T. Wang, D. G. Ouzounov, C. Wu, N. G. Horton, B. Zhang, C. H. Wu, Y. Zhang, M. J. Schnitzer, C. Xu, *Nat. Methods* **2018**, *15*, 789.
[7] A. Escobet-Montalbán, F. M. Gasparoli, J. Nylk, P. Liu, Z. Yang, K. Dholakia, *Opt. Lett.* **2018**, *43*, 5484.
[8] A. Vogel, V. Venugopalan, *Chem. Rev.* **2003**, *103*, 577.
[9] A. Vogel, J. Noack, G. Hüttman, G. Paltauf, *Appl. Phys. B* **2005**, *81*, 1015.
[10] A. A. Voronin, A. M. Zheltikov, *Phys. Rev. E* **2010**, *81*, 051918.
[11] A. A. Voronin, I. V. Fedotov, L. V. Doronina-Amitonova, O. I. Ivashkina, M. A. Zots, A. B. Fedotov, K. V. Anokhin, A. M. Zheltikov, *Opt. Lett.* **2011**, *36*, 508.
[12] L.-C. Cheng, N. G. Horton, K. Wang, S.-J. Chen, C. Xu, *Biomed. Opt. Express* **2014**, *5*, 3427.
[13] M. Drobizhev, N. S. Makarov, S. E. Tillo, T. E. Hughes, A. Rebane, *Nat. Methods* **2011**, *8*, 393.
[14] A. Rebane, A. Mikhaylov, in *Multiphoton Microscopy in the Biomedical Sciences XVIII*, International Society for Optics and Photonics, **2018**, vol. 10498, p. 1049830.
[15] A. A. Ivanov, A. A. Voronin, A. A. Lanin, D. A. Sidorov-Biryukov, A. B. Fedotov, A. M. Zheltikov, *Opt. Lett.* **2014**, *39*, 205.
[16] Y. G. Ermakova, V. V. Pak, Y. A. Bogdanova, A. A. Kotlobay, I. V. Yampolsky, A. G. Shokhina, A. S. Panova, R. A. Marygin, D. B. Staroverov, D. S. Bilan, *Chem. Commun.* **2018**, *54*, 2898.
[17] M. E. Matlashov, Y. A. Bogdanova, G. V. Ermakova, N. M. Mishina, Y. G. Ermakova, E. S. Nikitin, P. M. Balaban, S. Okabe, S. Lukyanov, G. Enikolopov, *Biochim. Biophys. Acta BBA-Gen. Subj.* **2015**, *1850*, 2318.
[18] M. S. Pochechuev, A. A. Lanin, I. V. Kelmanson, D. S. Bilan, D. A. Kotova, A. S. Chebotarev, V. Tarabykin, A. B. Fedotov, V. V. Belousov, A. M. Zheltikov, *Opt. Lett.* **2019**, *44*, 3166.
[19] M. Brenner, W. C. Kisseberth, Y. Su, F. Besnard, A. Messing, *J. Neurosci.* **1994**, *14*, 1030.
[20] S. Kügler, E. Kilic, M. Bähr, *Gene Ther.* **2003**, *10*, 337.
[21] N. S. Makarov, M. Drobizhev, A. Rebane, *Opt. Express* **2008**, *16*, 4029.
[22] H. Rabitz, R. de Vivie-Riedle, M. Motzkus, K. Kompa, *Science* **2000**, *288*, 5467.

## SUPPORTING INFORMATION

See supplementary material for a multimedia-view 3D reconstructions of Sypher3s-expressing neurons and astrocytes. Supporting Information may be found online in the supporting information tab for the article.

**Graphical abstract**

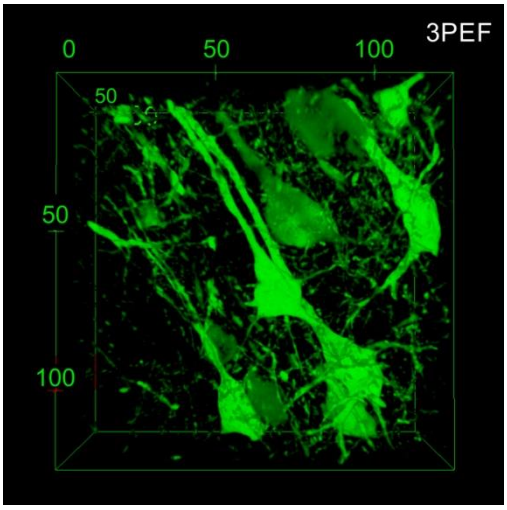


We demonstrate an accurate quantitative characterization of absolute two- and three-photon absorption (2PA and 3PA) action cross sections of a genetically encodable fluorescent marker Sypher3s. Both 2PA and 3PA action cross sections of this marker are found to be remarkably high, enabling high-brightness, cell-specific two- and three-photon fluorescence brain imaging.